

The Alkaloids of *Isatis indigotica* as Promising Candidates against COVID-19: A Molecular Docking Simulation for Drug Development

Abstract

Background: Due to the complexities of severe acute respiratory syndrome coronavirus 2 (SARS-CoV-2), an effective medicinal treatment protocol for this lethal disease with a high prevalence has not been approved yet. This study aimed to explore the efficacy of the main alkaloids of *Isatis indigotica*, one of the richest plant sources of alkaloids against SARS-CoV-2 targets computationally. **Materials and Methods:** 3D structures of the target proteins including 3CLpro; PLpro, and RdRp were downloaded from Protein Data Bank. The structures of ligands were retrieved from PubChem database or optimized by ORCA program. Ritonavir, Lopinavir, Sofosbuvir, and Remdesivir were selected as control inhibitors. Docking calculations were performed by AutoDock Vina option and top-ranked compounds were subjected to molecular dynamics simulation by Gromacs 5.1.4 simulation package. **Result:** The results showed that all 15 compounds had stronger interactions with PLpro in comparison to the other enzymes. Dihydroxylisopropylidenylisatisine A binds to the active site of PLpro with highest affinity (−9.3 kcal/mol) which is even more than the binding constants of Ritonavir and Lopinavir. Of the 15 compounds, Dihydroxylisopropylidenylisatisine A and Isatibisindosulfonic acid B had the highest tendency to bind to 3CLpro. Dihydroxylisopropylidenylisatisine A, Indirubin, Insatindibisindolamide A, Indigo, Insatindibisindolamide B, Isatibisindosulfonic acid B and Isatindosulfonic acid B had the highest RdRp binding affinity even more Remdesivir. **Conclusion:** Based on the results, the highest and weakest interaction with all three enzymes was observed for Dihydroxylisopropylidenylisatisine A and Epigoitrin, respectively. Based on these findings, Dihydroxylisopropylidenylisatisine A might be potential therapeutic candidate against SARS-CoV-2.

Keywords: Alkaloids, COVID-19, *isatis indigotica*, molecular docking analysis, molecular dynamic simulation, protease

Introduction

As the World Health Organization (WHO) announced the pandemic of coronavirus disease-2019 (COVID-19) on 11 March 2020, no effective treatment has been introduced to treat or eliminate the severe acute respiratory syndrome coronavirus (SARS-CoV-2). Besides, conventional medicines either do not have the necessary effectiveness or are used in higher doses to be effective, showing a wide range of side effects.^[1,2] On the contrary, due to their multi-targets character, phytochemicals have always been one of the options for discovering drug molecules to treat complicated diseases, including viral diseases and their complications.^[3] Therefore, the researchers have extensively designed and conducted *in-vitro*, *in-vivo*, and *in-silico* studies on natural compounds, including polyphenolic, terpenoid, coumarin,

and quinone derivatives against SARS-CoV-2.^[4] Based on these studies, alkaloids as nitrogenous natural compounds showed the prominent anti- SARS-CoV-2 activities via different mechanisms including interaction with enzymes involved in viral replication such as RNA dependent RNA polymerase (RdRp) and inhibition of two critical SARS-CoV-2 proteases including papain-like protease (PLpro), and 3-chymotrypsin-like protease (3CLpro). Also, these phytochemicals inhibited the structural proteins of SARS-CoV-2 such as spike and nucleocapsid proteins.^[5,6] For example, tetrandrine, fangchinoline, and, cepharanthine, as bisbenzylisoquinoline alkaloids of *Stephania tetrandra* (Menispermaceae), suppressed the expression of two vital structural proteins, spike (S) glycoprotein and nucleocapsid (N) protein, of human coronavirus strains OC43 (HCoV-OC43) at 5 μM.^[7] Also, Wink

This is an open access journal, and articles are distributed under the terms of the Creative Commons Attribution-NonCommercial-ShareAlike 4.0 License, which allows others to remix, tweak, and build upon the work non-commercially, as long as appropriate credit is given and the new creations are licensed under the identical terms.

For reprints contact: reprints@medknow.com

How to cite this article: Kazemi F, Mojarrab M, Bahrami G, Miraghaei SS, Hadidi S, Majnooni MB. The alkaloids of *Isatis indigotica* as promising candidates against COVID-19: A molecular docking simulation for drug development. J Rep Pharma Sci 2022;11:165-81.

Farnoosh Kazemi,
Mahdi Mojarrab¹,
Gholamreza Bahrami²,
Seyed Shahram
Miraghaei³,
Saba Hadidi⁴,
Mohammad Bagher
Majnooni⁵

Department of Biology, Faculty of Science, Razi University,
¹Pharmaceutical Sciences Research Center; Health Institute, Kermanshah University of Medical Sciences, ²Pharmaceutical Sciences Research Center; Health Institute, Kermanshah University of Medical Sciences, Kermanshah 6734667149, Iran and Medical Biology Research Center; Health Institute, Kermanshah University of Medical Sciences, ³Medical Biology Research Center; Health Institute, Kermanshah University of Medical Sciences, ⁴Department of Inorganic Chemistry, Faculty of Chemistry, Razi University, ⁵Kermanshah University of Medical Sciences, Kermanshah, Iran

Received: 11 Aug 2021

Accepted: 09 Feb 2022

Published: 23 Dec 2022

Address for correspondence:

Dr. Hadidi Saba,
Department of Inorganic Chemistry, Faculty of Chemistry, Razi University, Kermanshah, Iran.
E-mail: saba.hadidi@yahoo.com
Address for correspondence:
Dr. Majnooni Mohammad Bagher,
Student Research Committee, Kermanshah University of Medical Sciences, Kermanshah 6714415153, Iran.
E-mail: mb.majnooni64@yahoo.com

Access this article online

Website:

www.jrpsjournal.com

DOI:10.4103/jrptps.JRPTPS_113_21

Quick Response Code:



suggested the alkaloids with DNA interaction activities such as sanguinarine, berberine, palmatine, chelidonine, jatrorrhizine as a good candidate for anti- SARS-CoV-2 agents.^[8] On the contrary, the leaves and roots of *Isatis tinctoria* (synonymous with *Isatis indigotica*; Brassicaceae) are one of the rich sources of alkaloids from which more than 40 types of alkaloids, especially indole alkaloids, have been isolated.^[9,10] Also, several biological and pharmacological effects have been reported for *Isatis tinctoria* including analgesic, neuroprotective, cytotoxic, nitric oxide inhibitor, and anti-inflammatory effects.^[11-13] Besides, *Isatis tinctoria* showed anti-SARS-CoV *in-vitro* and *in-silico* studies. Lin and co-workers reported that the Indigo, Indirubin and, Indican, as indole alkaloids from *Isatis tinctoria* root, showed anti-SARS-CoV via the 3CLpro inhibition at 300 μ M, 293 μ M and, 112 μ M, respectively.^[14] Also, Ghosh and co-workers showed that the polyphenols of *Isatis tinctoria* root inhibited the RdRp and main proteases of SARS-CoV-2 in a docking study. In this study, the authors categorized indigo,

indirubin, and indican with alkaloid structure, and β -sitosterol, and emodin with terpenoid and quinone structure, respectively, as polyphenolic compounds that appear to be incorrect.^[15]

In this investigation, we applied a molecular docking study for interaction between indole alkaloids and alkaloids containing sulfur, as the two main categories of alkaloids isolated from *Isatis tinctoria* [Figure 1] with 3CLpro, PLpro, and RdRp of SARS-CoV-2 for the discovery of the new anti- SARS-CoV-2 drugs. In addition, ADMET (absorption, distribution, metabolism, excretion and toxicity) profiles of the top compounds that showed the best docking results for the target proteins were evaluated.

Materials and Methods

Protein and ligand preparation

For docking analysis, first, crystal structure of the target proteins including 3C-like protease (3CLpro; PDB ID: 6lu7),

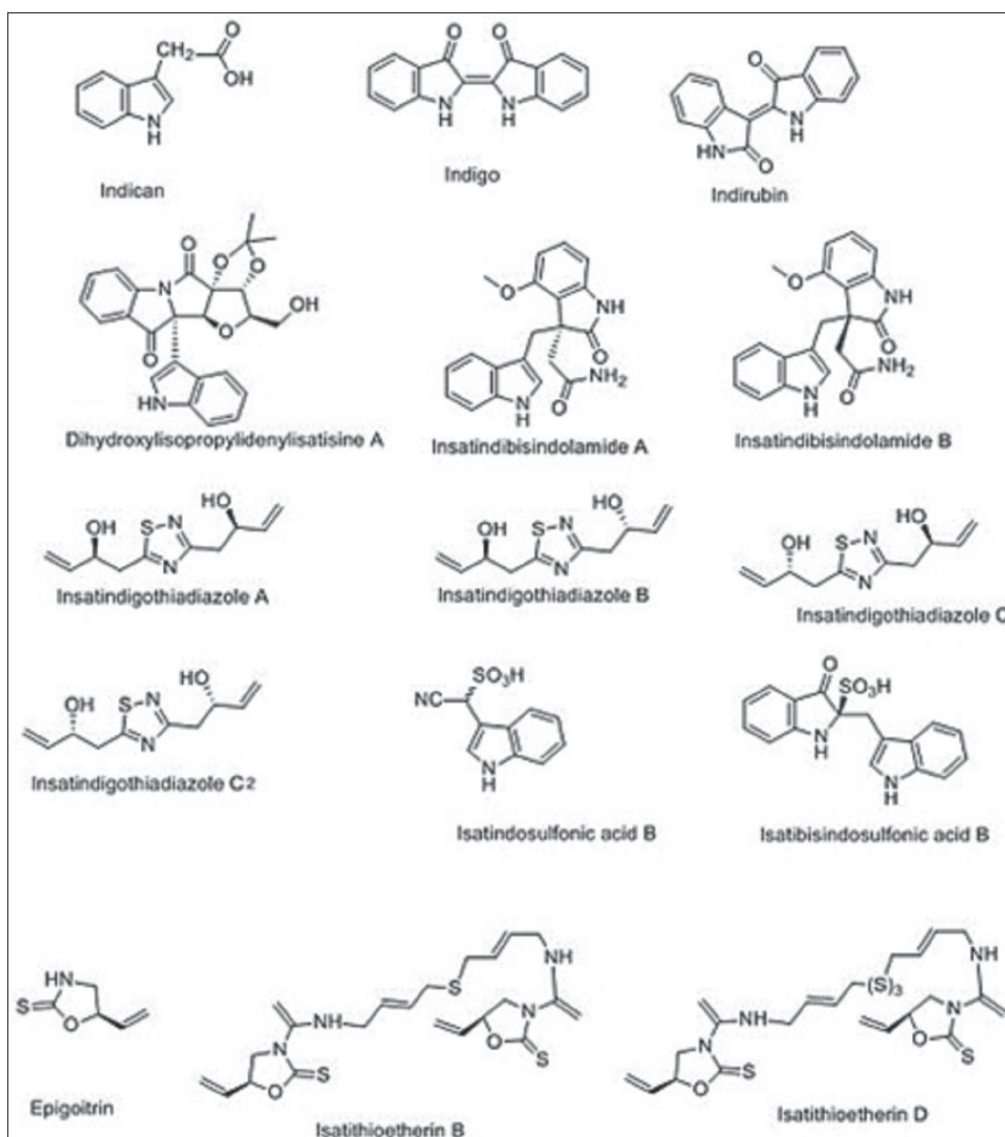


Figure 1: Chemical structure of 15 main substances of *Isatis indigotica*

papain-like protease (PLpro; PDB ID: 5y3e), and RNA dependent RNA polymerase (RdRp; PDB ID: 6m71) were obtained from Protein Data Bank (PDB).^[16] Co-crystallized ligands, cofactors, and water molecules were removed from the structures using BIOVIA Discovery Studio Visualizer 2016.^[17] The structures of 15 alkaloids from *Isatis indigotica* as ligands and the control inhibitors (Ritonavir, Lopinavir, Sofosbuvir, and Remdesivir) were retrieved from PubChem database or optimized by ORCA program.^[18] To prepare the structures, polar hydrogens were added and energy minimization was carried out using AutoDock Vina.

Molecular docking analysis

Docking calculations were performed by AutoDock Vina option based on scoring functions.^[19] For each target protein, the grid box was set to cover the active site residues. The remaining parameters were set as default. When calculations are done, results will be shown as the binding affinity (kcal/mol) values. The binding mode with the most negative binding affinity (highest affinity) was selected as the best mode for the corresponding ligand. After docking, LigPlot+ was used to plot bonding and nonbonding interactions of the ligand with the target protein in the protein–ligand complex.^[20]

Molecular dynamics simulation

The energy and structural properties of the ligand-protein complexes were determined through Gromacs 5.1.4 simulation package. The ligand-protein complex was inserted into a cubic box of 10 Å dimension and solvated using SPCE water model and the system was neutralized by adding Na⁺ or Cl⁻ ions and then the physiological cell environment was mimicked by adding 0.15 M of NaCl. The systems were simulated for 1000 ps^[21,22] in NPT ensemble at 310 K.

In silico ADMET studies

In this work, to evaluate ADMET profiles of the inhibitor ligands and the best alkaloids that showed significant binding affinities for the target proteins, their canonical SMILES were submitted to Swiss ADME and predicted pharmacokinetic parameters including gastrointestinal absorption (GIA), blood–brain barrier (BBB) permeability, P-glycoprotein (P-gp) substrate and CYP450 2C9 inhibitor were reported.^[23] Also, drug-likeness was investigated according to Lipinski's Rule of 5 (Ro5).^[24] Drug likeness assesses the chances for a molecule to become an oral drug with respect to bioavailability.^[23] In addition, to evaluate toxicity, carcinogenicity, and cardiotoxicity endpoint like human *Ether-a-go-go-related gene* (hERG) inhibition were predicted using admetSAR database.^[25]

Results

Molecular docking of selected ligands against PLpro (PDB ID: 5y3e)

SARS-CoV PLpro shares 82.8% sequence similarity with the homologous SARS-CoV-2 strain. Significantly, PLpro active site amino acids (Pro248, Pro249, Tyr269, Asp165, Glu168,

Leu163, Gly164, Gln270, Tyr274, Tyr265, and Thr302) of both strains are highly conserved. Thus, PLpro inhibitors of SARS-CoV may be potential inhibitors of SARS-CoV-2 PLpro enzyme.^[26] In order to identify selected ligands for treating SARS-CoV-2, the compounds were docked into the PLpro and compared with Lopinavir and Ritonavir as control inhibitors.^[27]

Lopinavir with binding affinity of –7.5 kcal/mol [Table 1] was attached to the active site of PLpro and interacted with Glu168, Tyr269, Gln270, and Arg167 by H-bond formation [Figure 2]. It contacted with Leu163, Tyr265, Tyr274, Pro249, Pro248, Asp165, and Gly164 via hydrophobic interactions. Ritonavir with binding affinity of –7.2 kcal/mol [Table 1] was attached to the active site of PLpro and formed 3 H-bonds with Tyr265, Asn268 and Gly272 [Figure 2]. Also it contacted with Thr302, Asp165, Pro248, Glu168, Tyr269, Pro249, Tyr274, Gly164, and Leu163 hydrophobically.

Indican with a binding affinity of –6.4 kcal/mol [Table 1] was attached to the active site of PLpro and formed o-bond with Tyr265. Furthermore, it contacted with Tyr269, Pro249, Thr302, and Asp165 via hydrophobic interactions [Figure 3]. Indigo with acceptable binding affinity of –8.5 kcal/mol [Table 1] was attached to the active site of PLpro and hydrophobically interacted with Glu168, Tyr265, Thr302, Asp165, and Pro249. In addition, one hydrogen bond was formed between O1 atom of Indigo and NH1 group of Arg167 [Figure 3]. Indirubin showed binding affinity of –8.3 kcal/mol against PLpro [Table 1], but it did not interact with the

Table 1: Binding affinities of the control inhibitors and the alkaloids from *Isatis indigotica* with the target proteins

Ligand	Binding affinity (kcal/mol)		
	5y3e	6lu7	6m71
Ritonavir	-7.2	-7.7	-
Lopinavir	-7.5	-7.4	-
Sofosbuvir	-	-	-6.4
Remdesivir	-	-	-6.0
Indican	-6.4	-5.6	-5.3
Indigo	-8.5	-7.3	-6.7
Indirubin	-8.3	-7.3	-7.7
Dihydroxyisopropylidenylisatisine A	-9.3	-8.5	-7.7
Insatindibisindolamide A	-7.8	-6.9	-7.1
Insatindibisindolamide B	-7.9	-6.9	-6.6
Insatindigothiadiazole A	-6.5	-5.4	-5.0
Insatindigothiadiazole B	-6.4	-5.4	-4.8
Insatindigothiadiazole C	-6.9	-5.3	-5.0
Insatindigothiadiazole C2	-6.4	-5.3	-4.7
Isatindosulfonic acid B	-7.1	-6.5	-6.2
Isatibisindosulfonic acid B	-8.3	-7.5	-6.5
Epigoitrin	-4.7	-3.9	-3.8
Isatithioetherin B	-6.3	-5.3	-5.7
Isatithioetherin D	-6.2	-5.4	-5.3

Not: Papain-like protease (PDB ID: 5y3e)

3C-like protease (PDB ID: 6lu7)

RNA polymerase (PDB ID: 6m71)

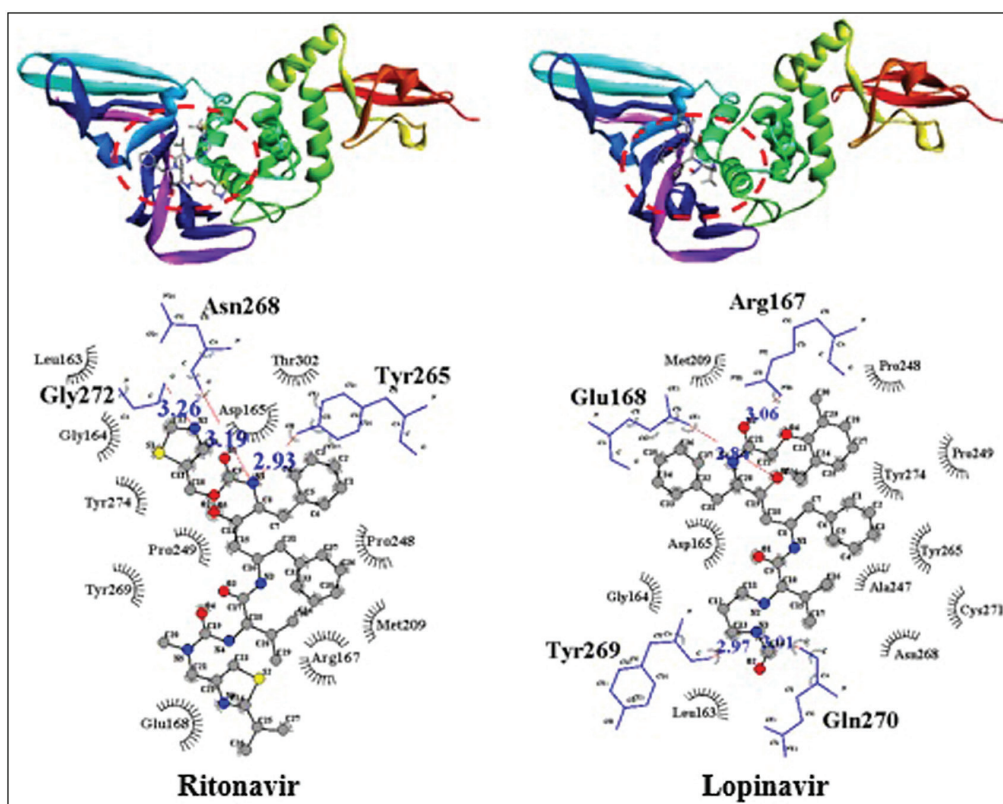


Figure 2: Docking simulation with the hydrogen and hydrophobic interactions between PLpro and control inhibitors

active site residues [Figure 3]. Top-ranked ligand of this study is Dihydroxylisopropylidenlisatisine A that strongly bound to PLpro (binding affinity: -9.3 kcal/mol, [Table 1]) and interacted with Tyr265 and Asn268 by H-bond formation and with Tyr274, Tyr269, Gly164 and Asp165 hydrophobically in the active site of this enzyme [Figure 3]. The docking results showed the crucial role of N2 at indole group in hydrogen bond formation. Insatindibisindolamide A with a binding affinity of -7.8 kcal/mol [Table 1] was attached to the active site of PLpro and formed 3 H-bonds with Tyr274, Gly164, and Gln270. Nitrogen of indole group in position 2 and amide nitrogen in position 3 are involved in H-bond formation. In addition, this compound interacted with Tyr269, Tyr265, Glu168, Thr302, Asp165, and Pro249 via hydrophobic interactions [Figure 3]. Insatindibisindolamide B showed binding affinity of -7.9 kcal/mol to PLpro [Table 1]. This compound formed one H-bond between O1 atom in carbonyl group and OH group of Tyr274. It also hydrophobically interacted with other active site residues including Pro249, Pro248, Asp165, Tyr265, Tyr269 [Figure 3]. Insatindigothiadiazole A with binding affinity of -6.5 kcal/mol [Table 1] was attached to the active site of PLpro and interacted with Tyr269, Tyr265 and Tyr274 with H-bond formation [Figure 3]. In addition, it contacted with Gln270, Pro249, Pro248 and Asp165 via hydrophobic interactions. Insatindigothiadiazole B with binding affinity of -6.4 kcal/mol [Table 1] was attached to the active site of PLpro and interacted with Tyr274 and Tyr265 with H-bond formation [Figure 3]. Also this compound contacted with Thr302, Pro249, Asp165,

Gln270, Leu163 and Gly164 via hydrophobic interactions. Insatindigothiadiazole C with binding affinity of -6.9 kcal/mol [Table 1] was attached to the active site of PLpro and interacted with Tyr269, Tyr274, Asp165, and Tyr265 through hydrogen bonds [Figure 3]. Other important residues that involved in binding of this compound are Pro248, Pro249, Thr302, and Gln270. Insatindigothiadiazole C2 showed binding affinity of -6.4 kcal/mol [Table 1] and interacted with the active site of PLpro by H-bond formation (Tyr265 and Tyr274) and hydrophobic interactions (Asp165, Thr302, Pro249, Gln270, and Leu163; [Figure 3]). Isatindosulfonic acid B bound to the active site of PLpro with a close binding affinity to Ritonavir (-7.1 kcal/mol, [Table 1]) and formed H-bond with Asp165. Moreover, it contacted with Tyr265, Pro249, and Tyr269 via hydrophobic interactions [Figure 3]. Isatibisindosulfonic acid B also showed more negative binding affinity (-8.3 kcal/mol) and consequently stronger binding compared to the control inhibitors including Ritonavir and Lopinavir [Table 1]. This compound was attached to the active site of PLpro through H-bond formation (Asp165 and Arg167) and hydrophobic interactions (Glu168, Pro249, Tyr265, and Thr302; [Figure 3]). Epigoitrin with binding affinity of -4.7 kcal/mol [Table 1] loosely bound to the active site of PLpro and contacted with Pro249, Asp165, Tyr274, Thr302, and Tyr265 hydrophobically [Figure 3]. Isatithioetherin B and Isatithioetherin D bound to PLpro with binding affinities of -6.3 and -6.2 kcal/mol, respectively [Table 1]. These two compounds did not interact with the active site residues [Figure 3].

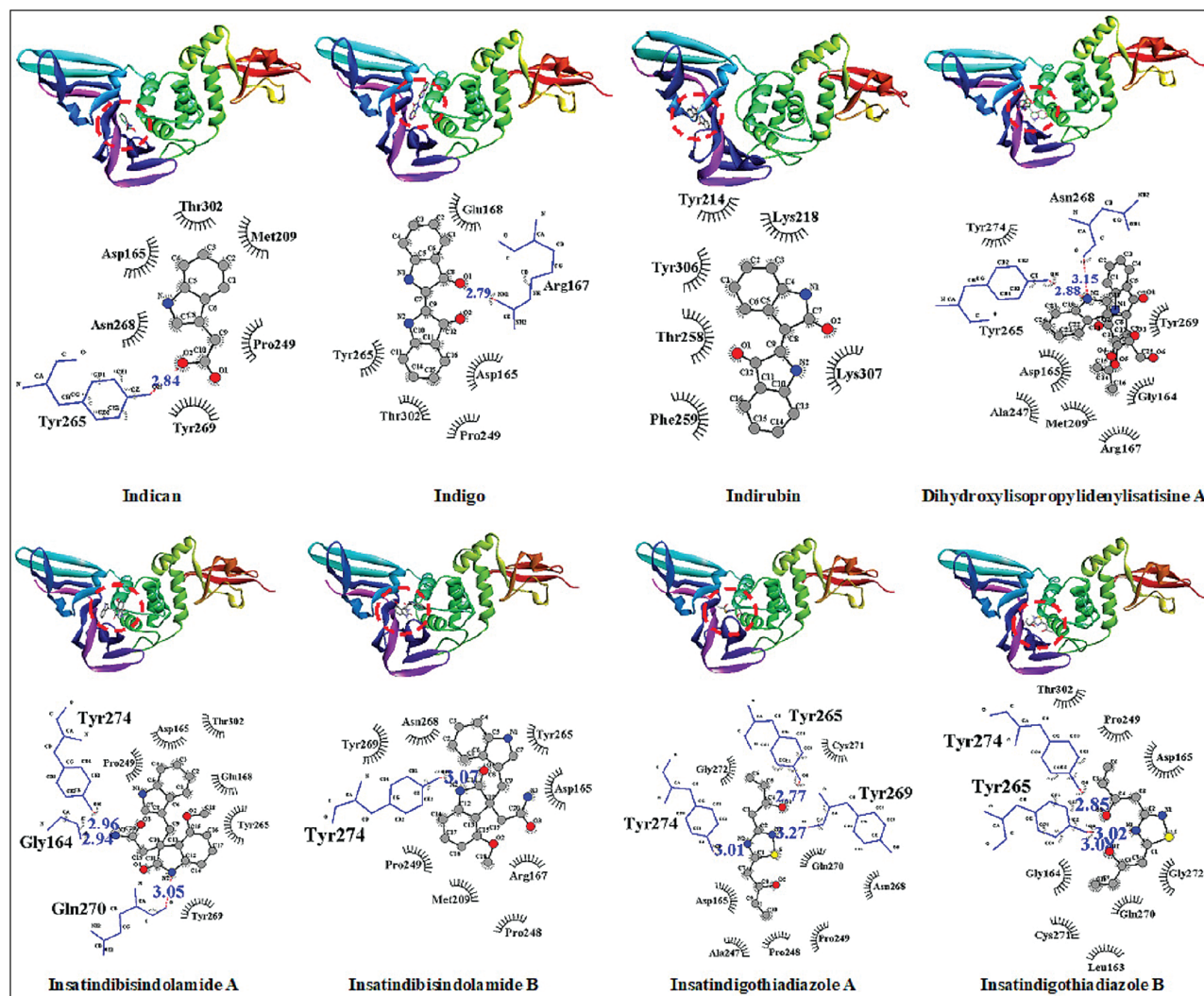


Figure 3: Docking simulation with the hydrogen and hydrophobic interactions between PLpro and the selected alkaloid ligands

Molecular docking of selected ligands against SARS-CoV-2 3CLpro (PDB ID: 6lu7)

3CLpro monomer has three domains, domain I (residues 8–101), domain II (residues 102–184), and domain III (residues 201–303), and a long loop (residues 185–200) connecting domain II and III. The active site of 3CLpro is located in the gap between domains I and II, and has a CysHis catalytic dyad (Cys145 and His41).^[28] In our study, the residues involved in the binding processes of all compounds were outside the Domain III [Figures 4 and 5]. The key residues that form the substrate-binding pocket of 3CLpro are Tyr54, His41, Met49, Asp187, Gln189, Phe185, Thr190, Ala191, Gln192, Pro168, Leu167, Glu166, His172, Met165, His164, Cys145, His163, Asn142, Leu141, Phe140, and Gly143.^[29]

Here, in addition to the 15 active compounds in *Isatis indigotica*, Lopinavir and Ritonavir were docked into 3CLpro as control inhibitor. The results are presented in [Table 2] and [Figures 4 and 5]. Ritonavir bound to binding pocket of 3CLpro with binding affinity of -7.7 kcal/mol [Table 1] and formed 4 H-bonds with Thr190, Asn142, Gln189, and Gly143 [Figure 4].

Also it contacted with the important residues including Asp187, His164, His41, Met49, Cys145, Phe140, Leu141, Glu166, and Met165 via hydrophobic interactions. As mentioned, in the active site of 3CLpro, a catalytic dyad consisting of His41 and Cys145 mediate protease activity. Therefore, these interactions may disrupt the activity of Cys145-His41 catalytic dyad.^[30] Another control inhibitor, Lopinavir with binding affinity of -7.4 kcal/mol [Table 1] was attached to the binding pocket of 3CLpro and interacted with Gln189 and Thr45 through H-bond formation. In addition, it contacted with Met49, His41, Asp187, Thr190, Pro168, His164, Phe140, His163, Glu166, Met165, and Gly143 via hydrophobic interactions [Figure 4].

Indican in comparison to the control inhibitors was weakly attached to the binding pocket of 3CLpro (binding affinity: -5.6 kcal/mol; [Table 1]) and it interacted with the residues of domain II including Gly143, Cys145, and Ser144 via H-bond formation and with Asn142, His163, Phe140, Leu141 and Glu166 as hydrophobic interactions [Figure 5]. Indigo and Indirubin both with binding affinity of -7.3 kcal/mol were attached to 3CLpro [Table 1]. Indigo did not form any hydrogen bond,

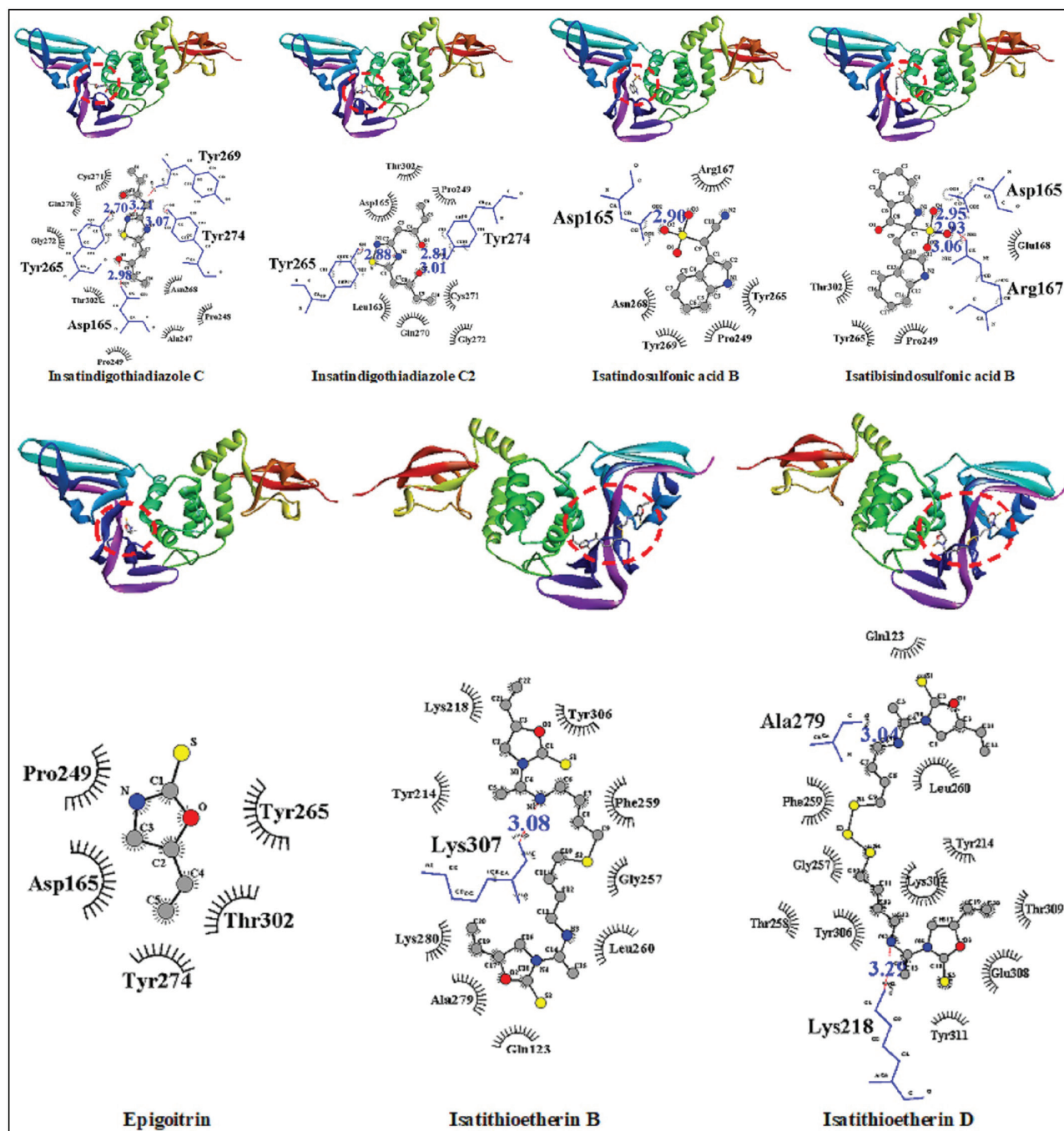


Figure 3: Continued

but with hydrophobic interactions connected to the binding pocket (Gln189, Asp187, His41, Met165, Glu166, Phe140, Leu141, His164, and Asn142; [Figure 5]). Whereas, Indirubin interacted with Cys145 and Ser144 through 3 H-bonds and with Leu141, Glu166, Gly143, Asn142, His163 (in domain II), and Met49 (in domain I) as hydrophobic interactions [Figure 5]. Dihydroxyisopropylidenylisatisine A with highest affinity was attached to the binding pocket of 3CLpro (binding affinity of -8.5 kcal/mol; [Table 1]). This compound interacted with the key residues including His164, Met165, Gly143, Asn142, Phe140, Glu166, Cys145, His163, Leu141 (in domain

II), and Gln189 (in long loop connecting domain II and III) hydrophobically [Figure 5]. Insatindibisindolamide A with binding affinity of -6.9 kcal/mol was attached to binding pocket of 3CLpro [Table 1]. It interacted with His163 and Glu166 through H-bond formation. Also this compound interacted with Met165, His41, His164, Gln189, Cys145, Asn142, Phe140, Leu141, Gly143, and His172 hydrophobically [Figure 5]. Insatindibisindolamide B with binding affinity of -6.9 kcal/mol was attached to 3CLpro [Table 1] and interacted with binding pocket through hydrogen bonds (Glu166 and His163) and hydrophobic interactions (Gln189, His172, Met165, His164,

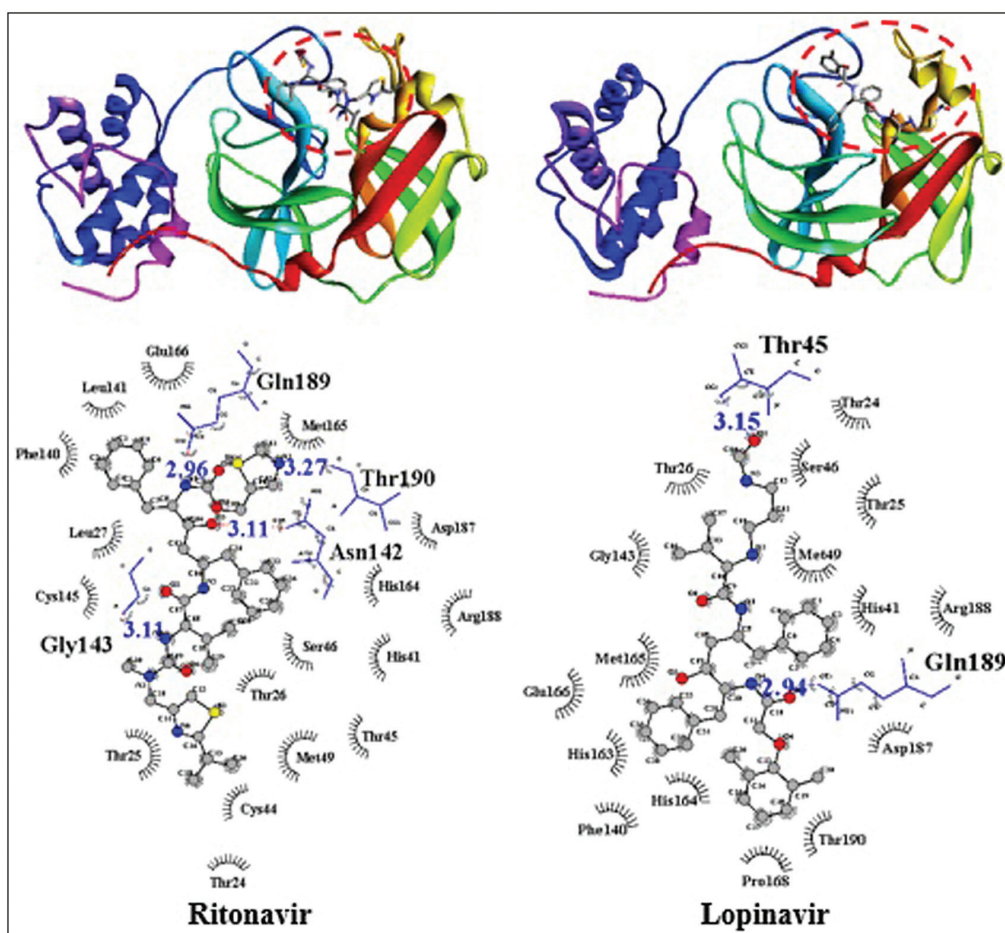


Figure 4: Docking simulation with the hydrogen and hydrophobic interactions between 3CLpro and control inhibitors

His41, Cys145, Met165, Asn142, Leu141, and Phe140; [Figure 5]). Insatindigothiadiazole A with binding affinity of -5.4 kcal/mol [Table 1] was attached to the binding pocket of 3CLpro and formed 3 H-bonds with His164, His163 and Gln189 [Figure 5]. In addition, it contacted with Asp187, Met49, Met165, Glu166, Leu141, Phe140, His41, and Cys145 via hydrophobic interactions. Insatindigothiadiazole B also bound to the binding pocket of 3CLpro with binding affinity of -5.4 kcal/mol [Table 1] and interacted with Leu141 and His164 via H-bond formation and with Phe140, Glu166, Cys145, Asp187, Gln189, His41, Met165, and His163 hydrophobically [Figure 5]. Insatindigothiadiazole C with binding affinity of -5.3 kcal/mol [Table 1] was attached to the binding pocket of 3CLpro and formed 2 H-bonds with Gln189 and His163 [Figure 5]. Moreover, it contacted with Phe140, Cys145, Glu166, Leu141, Asn142, Met165, Asp187, Met49, Tyr54, His41, and His164 via hydrophobic interactions. Insatindigothiadiazole C2 bound to binding pocket of 3CLpro with binding affinity of -5.3 kcal/mol [Table 1] and formed 3 H-bonds with Gln189, His164, Leu141 [Figure 5]. This compound contacted with Met49, His41, Asp187, Met165, Cys145, Glu166, His163, and Phe140 via hydrophobic interactions. Isatindosulfonic acid B with binding affinity of -6.5 kcal/mol [Table 1] interacted with Leu141, Ser144 and His163 via H-bond formation [Figure 5]. Additionally, it

interacted hydrophobically with other key residues in binding pocket of 3CLpro (Asn142, Cys145, His164, Gly143, Met165, Gln189, Glu166 and Phe140). Isatibisindosulfonic acid B with binding affinity of -7.5 kcal/mol [Table 1] was attached to the binding pocket of 3CLpro through hydrogen bonds (Leu141 and His163) and hydrophobic interactions (Met165, Gln189, Gly143, Met49, Cys145, Asn142, and His164, [Figure 5]). The weakest connection is related to Epigoitrin with binding affinity of -3.9 kcal/mol [Table 1] that hydrophobically interacted with Gln189, Met49, His41, Tyr54, Asp187, Met165, and His164 [Figure 5]. Isatithioetherin B and Isatithioetherin D were attached to the binding pocket of 3CLpro with binding affinity of -5.3 and -5.4 kcal/mol, respectively [Table 1]. Both compounds interacted with His164 through H-bond formation and with Met49, Gly143, Gln189, Asn142, Met165, and His41 hydrophobically [Figure 5]. Isatithioetherin B also interacted with Leu141, Phe140, His163, His172, and Glu166. Other important residues in binding of Isatithioetherin D are Tyr54, Asp187, and Cys145.

Molecular docking of selected ligands against RdRp (PDB ID: 6m71)

RdRp is composed of three subdomains including finger domain (residues 398–581, 628–687), palm domain (582–627, 688–815), and thumb domain (816–919).^[31,32] The active site

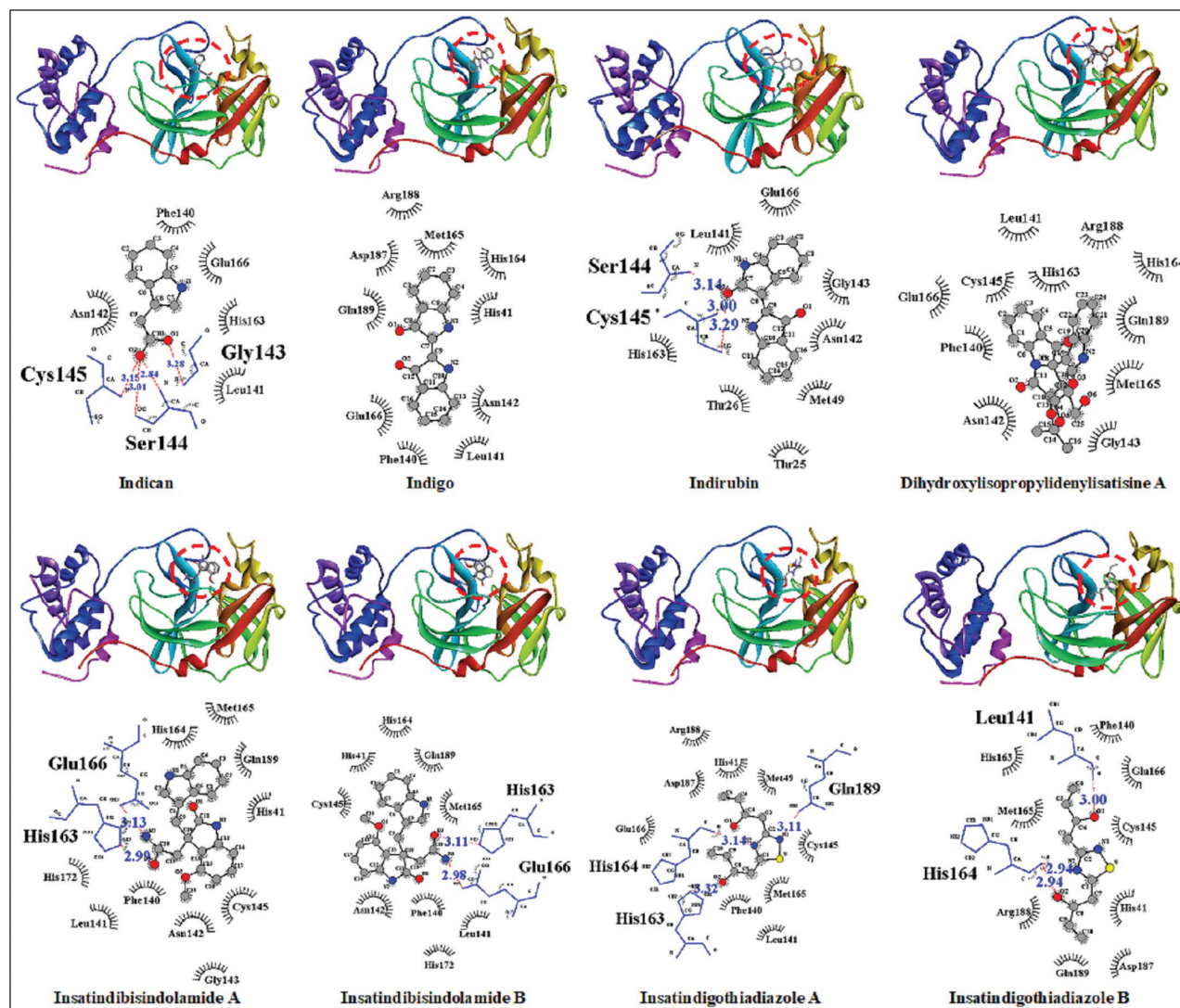


Figure 5: Docking simulation with the hydrogen and hydrophobic interactions between 3CLpro and the selected alkaloid ligands

key residues that are located on the palm domain are adjacent aspartates, that is, Asp760 and Asp761, which are involved in the actual reaction of the RdRp enzyme.^[32-34] Also, the key residues surrounding the active site aspartates that are highly conserved include; Tyr619, Cys622, Asn691, Asn695, Met755, Ile757, Leu758, Ser759, Ala762, Val763, Glu811, Phe812, Cys813, and Ser814.^[31,34] Drugs Sofosbuvir and Remdesivir as controls along with 15 active compounds in *Isatis indigotica* as candidate ligands were docked to investigate interaction with RdRp.

Sofosbuvir bound to RdRp with binding affinity of -6.4 kcal/mol [Table 1] and interacted with Glu811, Ser814, Cys813, and Trp800 through hydrogen bonds. In addition, it interacted with Asp761 and Phe812 hydrophobically [Figure 6]. Remdesivir with binding affinity of -6.0 kcal/mol [Table 1] bound to the active site of RdRp through hydrogen bond (Asp760 and Lys798) and hydrophobic interaction (Asp761). Other key residues that interacted with Remdesivir include Glu811, Asp618, and Ser814 [Figure 6].

Indican with binding affinity of -5.3 kcal/mol [Table 1] was attached to RdRp palm domain and interacted with Asp761 hydrophobically [Figure 7]. Also it interacted with important residues including Asp618 and Glu811 via hydrophobic interactions and one hydrogen bond was formed between O atom of Indican and Trp800 residue (NH group). Indigo bound to RdRp through hydrogen bonding and hydrophobic interactions (binding affinity: -6.7 kcal/mol). However, it could not interact with the active site residues [Table 1 and Figure 7]. Indirubin showed better binding affinity (-7.7 kcal/mol) than Sofosbuvir and Remdesivir and interacted with Asp761 and Asp760 by hydrogen bond and hydrophobic interaction, respectively [Table 1 and Figure 7]. Also, it hydrophobically interacted with Asp618 and Glu811. Dihydroxylisopropylidenylisatisine A like Indirubin showed binding affinity of -7.7 kcal/mol and bound to palm domain by hydrogen bonding and hydrophobic interactions but did not interact with the active site aspartates [Table 1 and Figure 7]. Insatindibisindolamide A with binding affinity of -7.1 kcal/mol was attached to RdRp and interacted with Asp761,

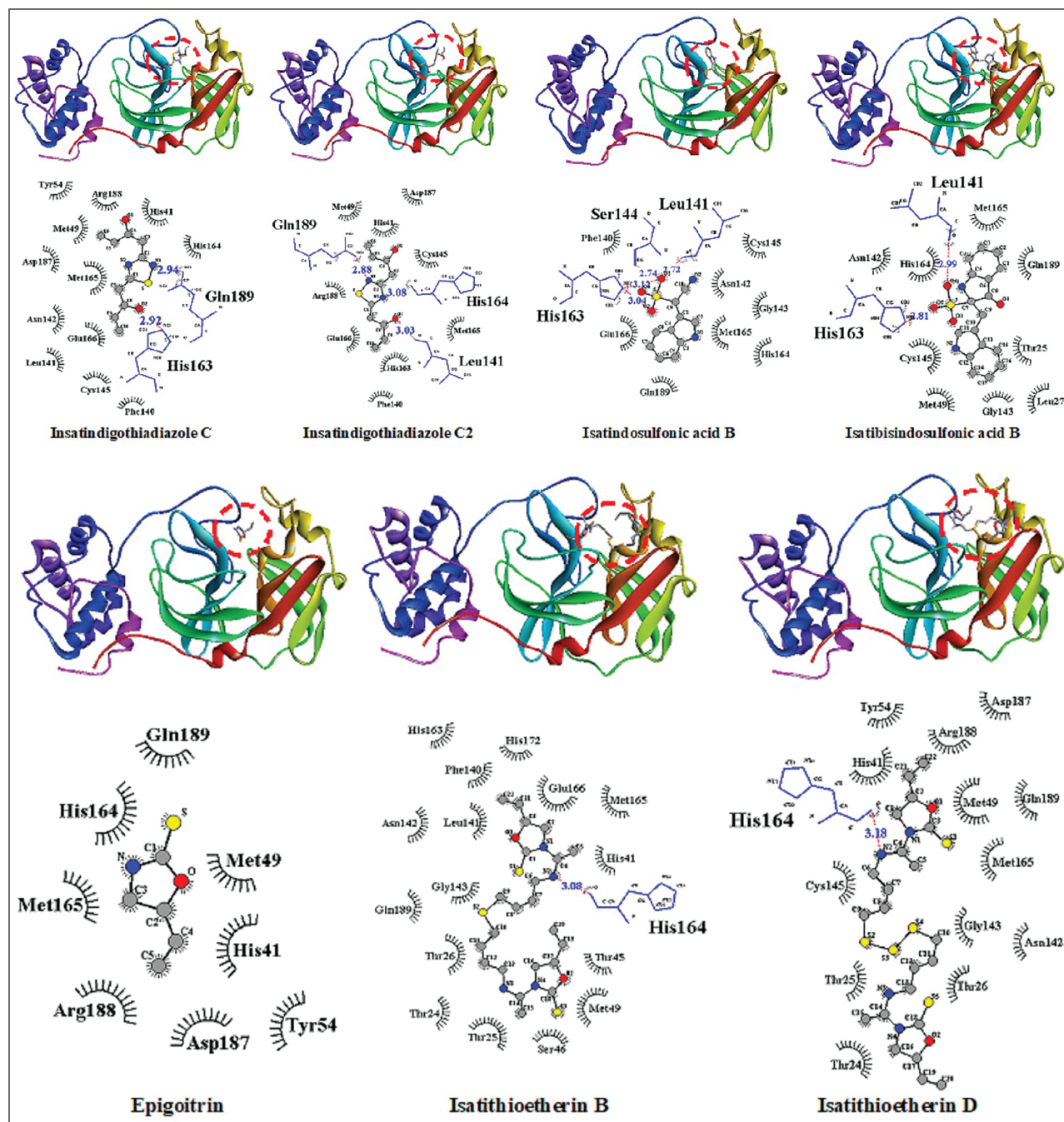


Figure 5: Continued

Table 2: Drug-likeness prediction through SwissADME

Ligand	MW (g/mol) (≤500)	HBA (≤10)	HBD (≤5)	MLOGP	TPSA (Å ²)	Lipinski's violation
Ritonavir	720.94	7	4	1.80	202.26	1 violation: MW>500
Lopinavir	628.80	5	4	2.93	120.00	1 violation: MW>500
Sofosbuvir	529.45	11	3	0.82	167.99	2 violations: MW>500, NorO>10
Remdesivir	602.58	12	4	0.18	213.36	2 violations: MW>500, NorO>10
Indigo	262.26	3	2	1.29	65.45	0
Indirubin	262.26	3	2	1.70	65.45	0
Dihydroxylisopropylidenylisatisine A	446.45	6	2	0.62	101.09	0
Isatibisindosulfonic acid B	342.37	4	3	1.18	107.64	0

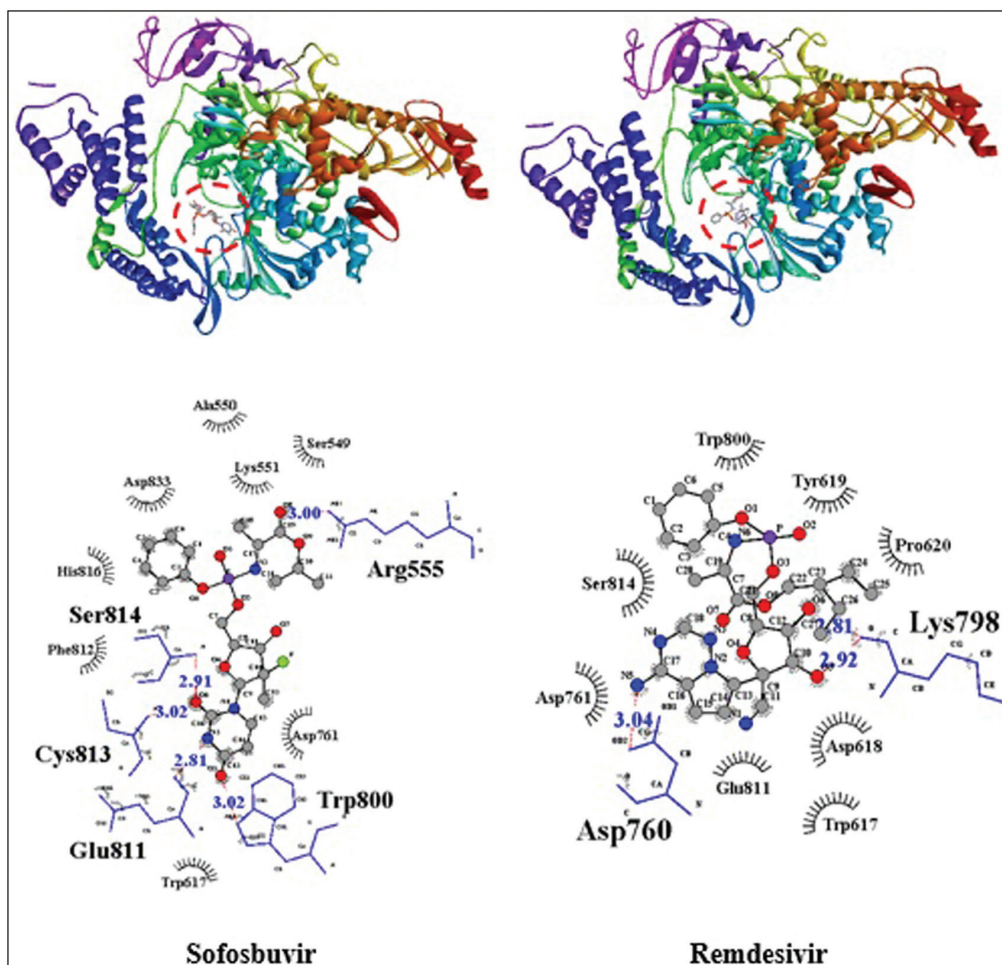


Figure 6: Docking simulation with the hydrogen and hydrophobic interactions between RdRp and control inhibitors

Glu811, Trp617, and Trp800 by H-bond formation [Table 1 and Figure 7]. Other important residues involved in binding of this compound are Asp760 and Asp618. Insatindibisindolamide B with binding affinity of -6.6 kcal/mol [Table 1] was attached to RdRp and interacted with Asp761 and Trp617 by H-bond formation [Figure 7]. Also it contacted with Asp760, Asp618, and Glu811 hydrophobically. Insatindigothiadiazole A showed binding affinity of -5.0 kcal/mol [Table 1] and interacted with Asp761 hydrophobically. This compound interacted with Glu811, Lys798, and Ser814 by H-bond formation and with Cys813 hydrophobically [Figure 7]. Insatindigothiadiazole B also bound to palm domain of RdRp through hydrogen bonds and hydrophobic interactions (binding affinity: -4.8 kcal/mol), but did not interact with the active site aspartates [Figure 7]. Insatindigothiadiazole C with binding affinity of -5.0 kcal/mol was attached to RdRp and interacted with Asp761, Cys813, Ser814 and Glu811 via hydrophobic interactions [Table 1 and Figure 7]. Insatindigothiadiazole C2 also with binding affinity of -4.7 kcal/mol [Table 1] bound to RdRp and interacted with Asp761 and Glu811 by H-bond formation and with Asp760 and Asp618 via hydrophobic interactions [Figure 7]. Isatindosulfonic acid B with binding affinity of -6.2 kcal/mol was attached to RdRp [Table 1] and interacted with some key residues through hydrogen bond (Glu811) and hydrophobic

interactions (Asp760, Asp761, Ser814, Phe812, and Asp618; [Figure 7]). Isatibisindosulfonic acid B with binding affinity of -6.5 kcal/mol was attached to RdRp and formed 4 H-bonds with Asp761, Ser814, Glu811, and Asp618 [Table 1 and Figure 7]. Also it contacted with Asp760 and Phe812 hydrophobically. Epigoitrin weakly bound to RdRp with binding affinity of -3.8 kcal/mol and could not interact with the active site aspartates [Table 1 and Figure 7]. Isatithioetherin B bound to palm domain of RdRp with binding affinity of -5.7 kcal/mol and interacted with Cys622 and Tyr619 by H-bond formation [Table 1 and Figure 7]. This compound contacted with Asp761, Glu811, and Asp618 via hydrophobic interactions. Isatithioetherin D bound to palm domain of RdRp with binding affinity of -5.3 kcal/mol, but did not interact with the active site aspartates [Table 1 and Figure 7].

Molecular dynamics simulation of PLpro-Dihydroxyisopropylidenylsatisstine A

The molecular dynamics simulation was carried out for the most promising compounds Dihydroxyisopropylidenylsatisstine A against PLpro and 3CLpro and Indirubin against RdRp.

The total range of potential energy changes was between $-1225,500$ and $-1219,500$ kJ/mol at 0 to 1000 ps and the major

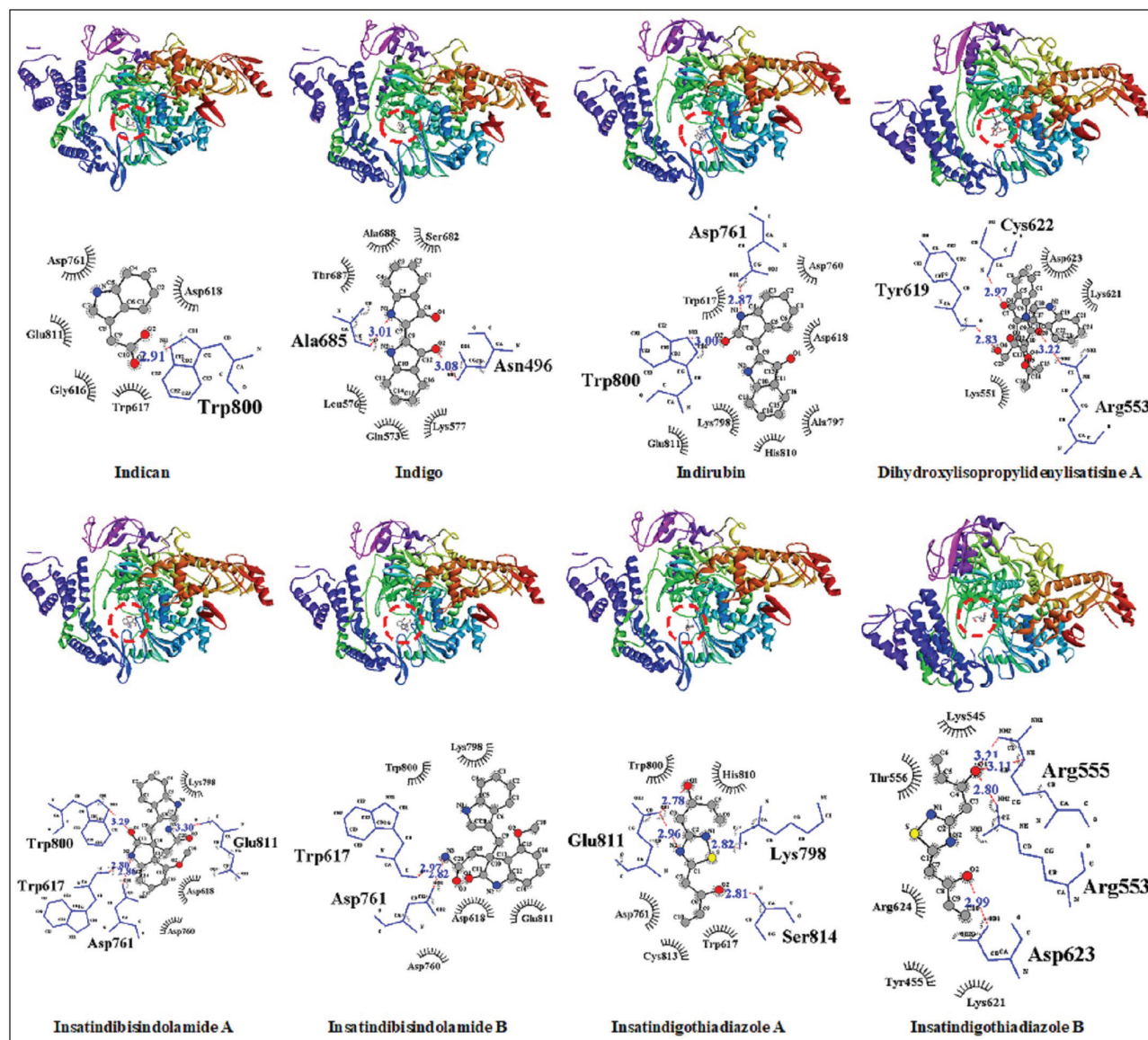


Figure 7: Docking simulation with the hydrogen and hydrophobic interactions between RdRp and the selected alkaloid ligands

range of potential energy changes was between $-1223,500$ and $-1221,000$ kJ/mol [Figure 8A]. Also, the total range of changes related to kinetic energy was between $203,000$ and $207,500$ kJ/mol and the main range of changes related to kinetic energy was between $204,000$ and $206,500$ kJ/mol [Figure 8B]. Finally, the total range of changes related to total energy was between $-1019,400$ and $-1015,600$ kJ/mol and the main range of changes related to total energy was between $-1017,200$ and $-1016,400$ kJ/mol [Figure 8C]. The range for system RMSD was between 0.2675 and 0.3175 in the frames $0-1100$, which indicates that the accuracy of the relevant calculations was high, because the values are close to zero, and whatever be close to zero indicate the high accuracy of calculations and the selection of the appropriate force field. Also, the range for protein RMSD is between 0.255 and 0.295 , which again indicates the high accuracy of the calculations [Figure 8D]. As can be seen in the potential energy diagram near 50 ps had the lowest amount of

energy due to proper docking, then, in a period of about 100 ps, we see the highest amount of potential energy (more positive), which is the lowest value in the kinetic energy diagram and again shows the inverse relationship between potential energy and kinetic energy, then the suffering associated with potential energy changes is constant and equilibrium. Also in the total energy diagram, in the early times of molecular dynamics, we see the lowest amount of total energy, which indicates that the docking used for molecular dynamics was in the best condition and the system was in good stability, then at 600 ps the total energy had the highest value (more positive) that the system went to instability, which can also be seen in the potential energy diagram, at which time the potential energy also became more (more positive) and the kinetic energy had its lowest value, after that, in a time of nearly 1000 ps, the energy of the total system decreases until the system reaches the necessary stability, after which it achieves the system balance.

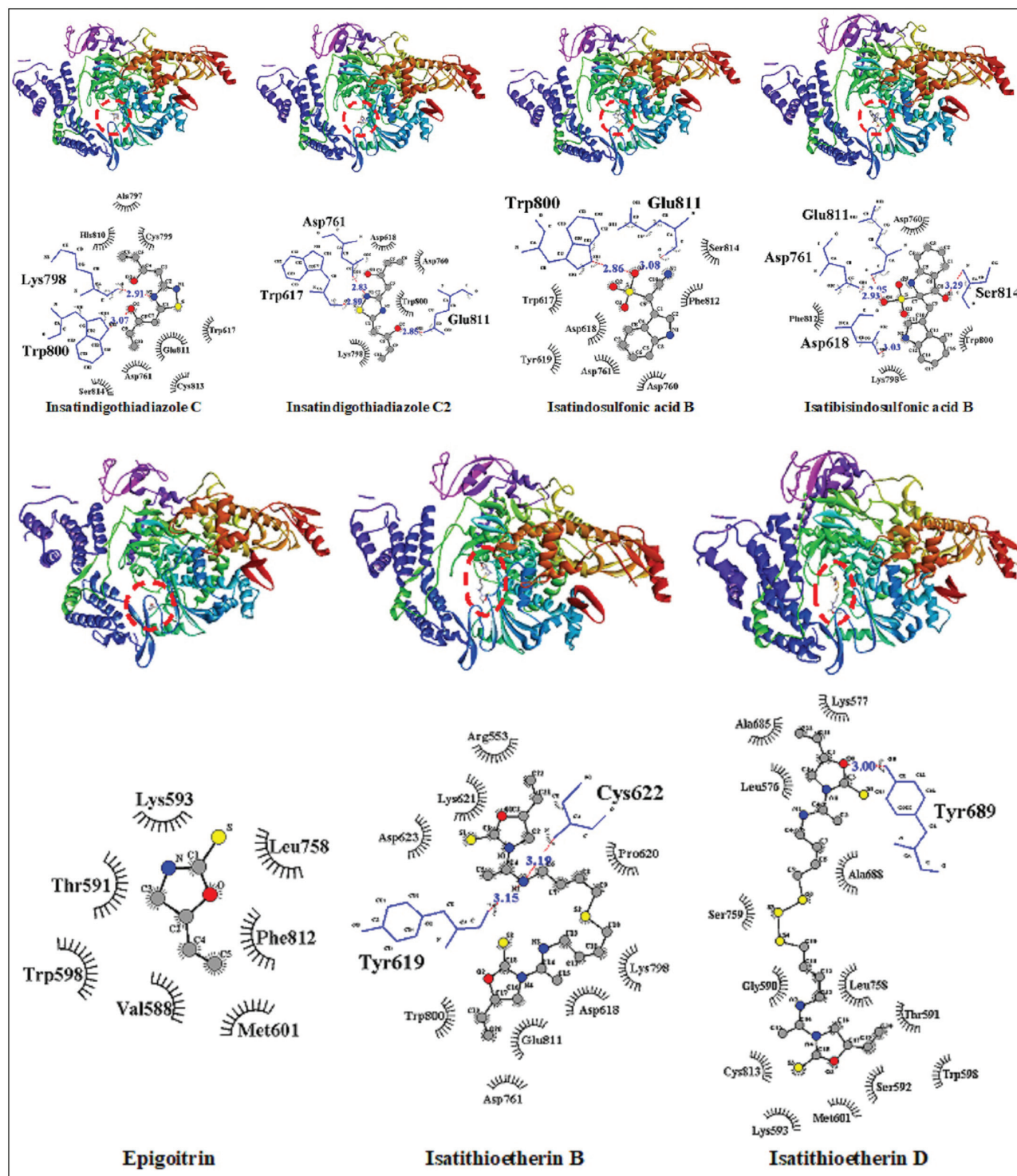


Figure 7: Continued

Molecular dynamics simulation of 3CLpro-dihydroxylisopropylidenylsatistine A

The total range of potential energy changes was between -1276,500 and -1270,500 kJ/mol at 0–1000 ps and the major range of potential energy changes was between -1274,500 and -1272,000 kJ/mol [Figure 9A]. Also, the total range of changes related to kinetic energy was between 202,000 and

206,500 kJ/mol and the main range of changes related to kinetic energy was between 203,000 and 205,500 kJ/mol [Figure 9B]. Finally, the total range of changes related to total energy was between -1070,400 and -1068,000 kJ/mol and the main range of changes related to total energy was between -1069,600 and -1069,000 kJ/mol [Figure 9C]. The range for system RMSD was between 0.2525 and 0.3025 in the frames 0–1100, which

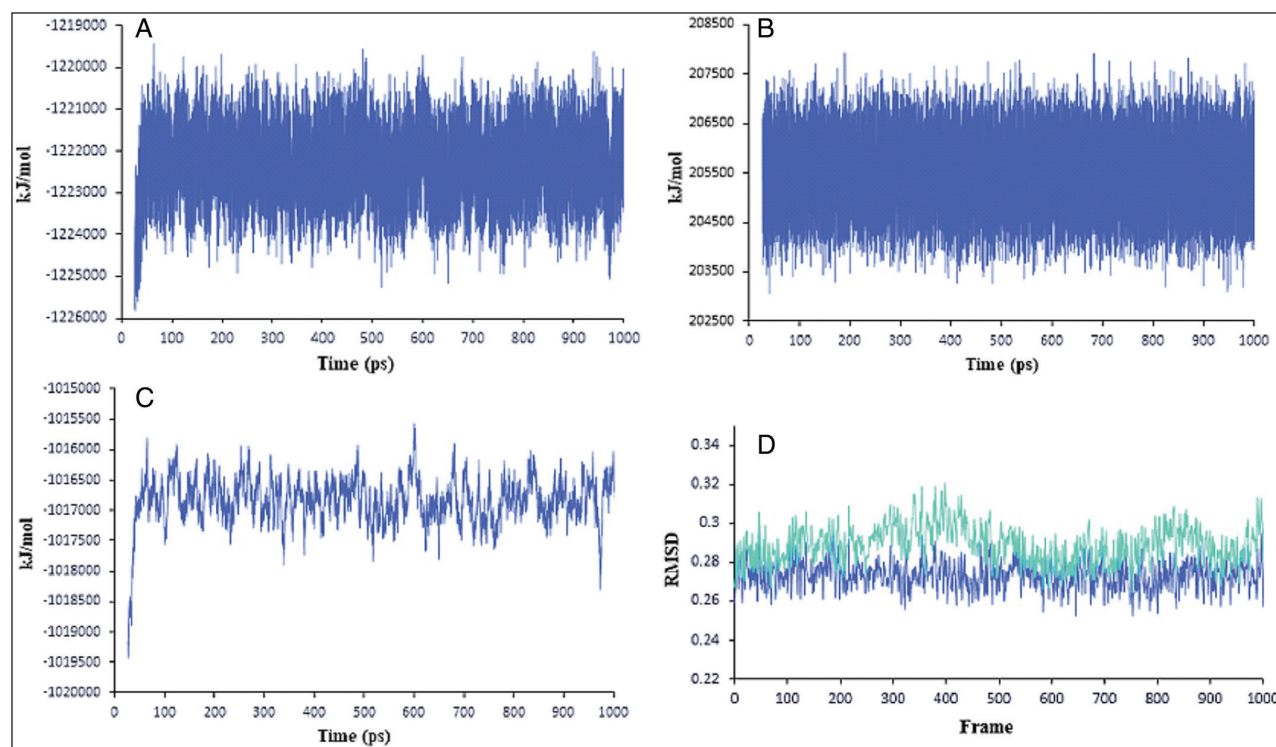


Figure 8: Analysis of MD trajectories for PLpro-Dihydroxylisopropylidenylisatisine A complex (A) potential energy, (B) kinetic energy, (C) total energy and (D) RMSD of protein backbone (blue line) and system (green line)

indicates that the accuracy of the relevant calculations was high. Also, the range for protein RMSD is between 0.24 and 0.29, which again indicates the high accuracy of the calculations [Figure 9D]. The changes in potential energy were almost constant, but at about 200 ps the potential energy had its lowest value (negative), that is, it was stable, which at the same time showed the highest amount of kinetic energy. This result indicates that there is an inverse relationship between potential energy and kinetic energy, also, the total system energy shows its lowest value close to 200 ps time, indicating that there is an almost direct relationship between the potential energy and the total system energy. At 550 and 900 ps, the potential energy has reached its maximum (more positive) and the system is destabilizing, and at these times, kinetic energy has shown its lowest value, which indicates the inverse relationship between potential energy and kinetic energy, also, in the same time intervals, the energy of the total system has the highest value (more positive), which indicates that the system is unstable. After 900 ps, the system goes into equilibrium and the potential and total energies are almost constant and go negative until the system reaches the required stability.

Molecular dynamics simulation of RdRp-indirubin

The total range of potential energy changes was between $-1258,000$ and $-1251,000$ kJ/mol at 0–1000 ps and the major range of potential energy changes was between $-1254,500$ and $-1252,500$ kJ/mol [Figure 10A]. Also, the total range of changes related to kinetic energy was between 221,500 and 227,000 kJ/mol and the main range of changes related

to kinetic energy was between 223,000 and 226,000 kJ/mol [Figure 10B]. Finally, the total range of changes related to total energy was between $-1032,500$ and $-1028,000$ kJ/mol and the main range of changes related to total energy was between $-1030,500$ and $-1029,500$ kJ/mol [Figure 10C]. The range for system RMSD was between 0.3075 and 0.3525 in the 0–1100 frames, indicating that the accuracy of the relevant calculations was high. Also, the range for protein RMSD is between 0.235 and 0.285, which again indicates the high accuracy of the calculations [Figure 10D]. In the potential energy diagram, in the initial time periods, the lowest amount of energy and the highest amount of it can be seen, which indicates proper docking and balancing of the system, From approximately 0 - 500 ps, the system shows large changes in energy, with potential energy being directly related to total energy and inversely related to kinetic energy, After a time of 500 ps, the system of suffering related to its energy changes is constant and goes towards equilibrium.

ADME analysis

[Table 2] shows the drug-likeness of the control inhibitors and the top docked compounds (Dihydroxylisopropylidenylisatisine A, Indigo and Isatibisindosulfonic acid B for PLpro; Dihydroxylisopropylidenylisatisine A for 3CLpro; Indirubin for RdRp). To determine whether any compound with a particular biological activity has the potential to serve as a pharmacological agent/drug, the Lipinski rule of five is generally used in which an orally bioactive drug is expected not to violate more than one of the criteria for drug-likeness.^[35,36]

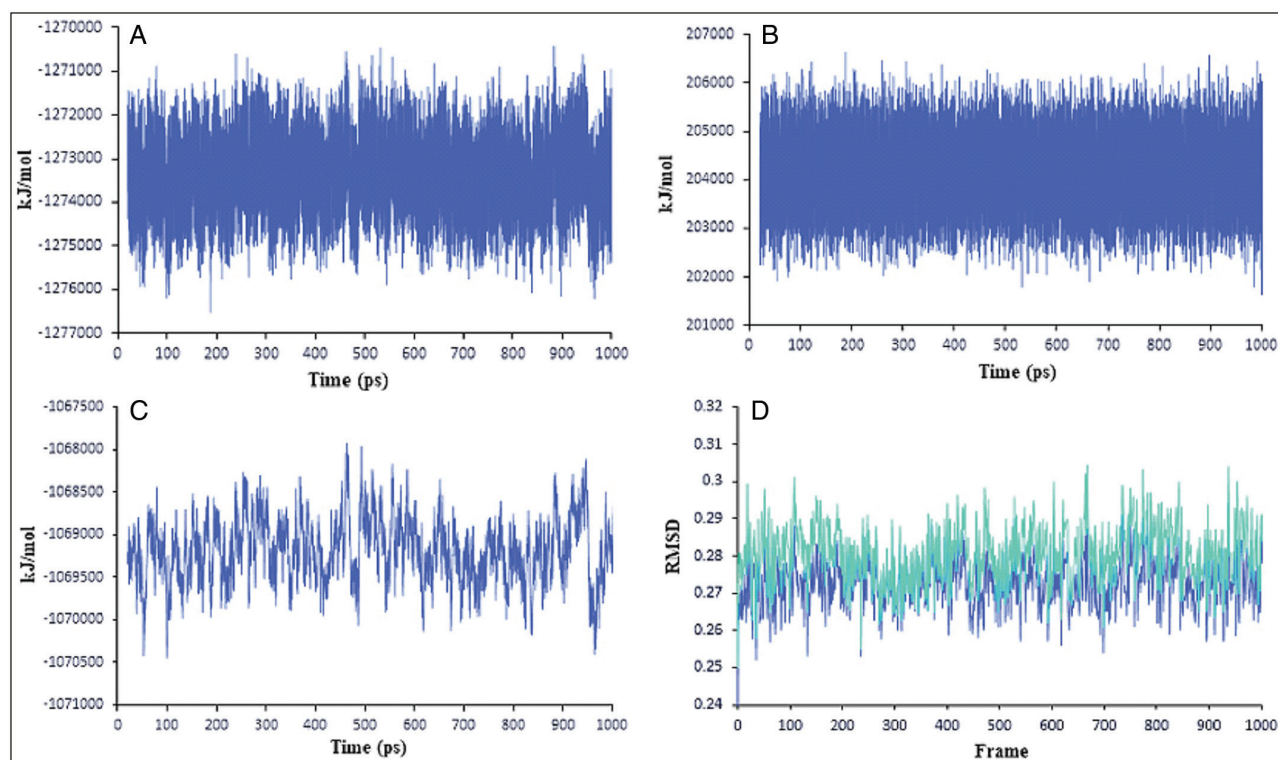


Figure 9: Analysis of MD trajectories for 3CLpro-Dihydroxylisopropylidenylsatisstine A complex (A) potential energy, (B) kinetic energy, (C) total energy and (D) RMSD of protein backbone (blue line) and system (green line)

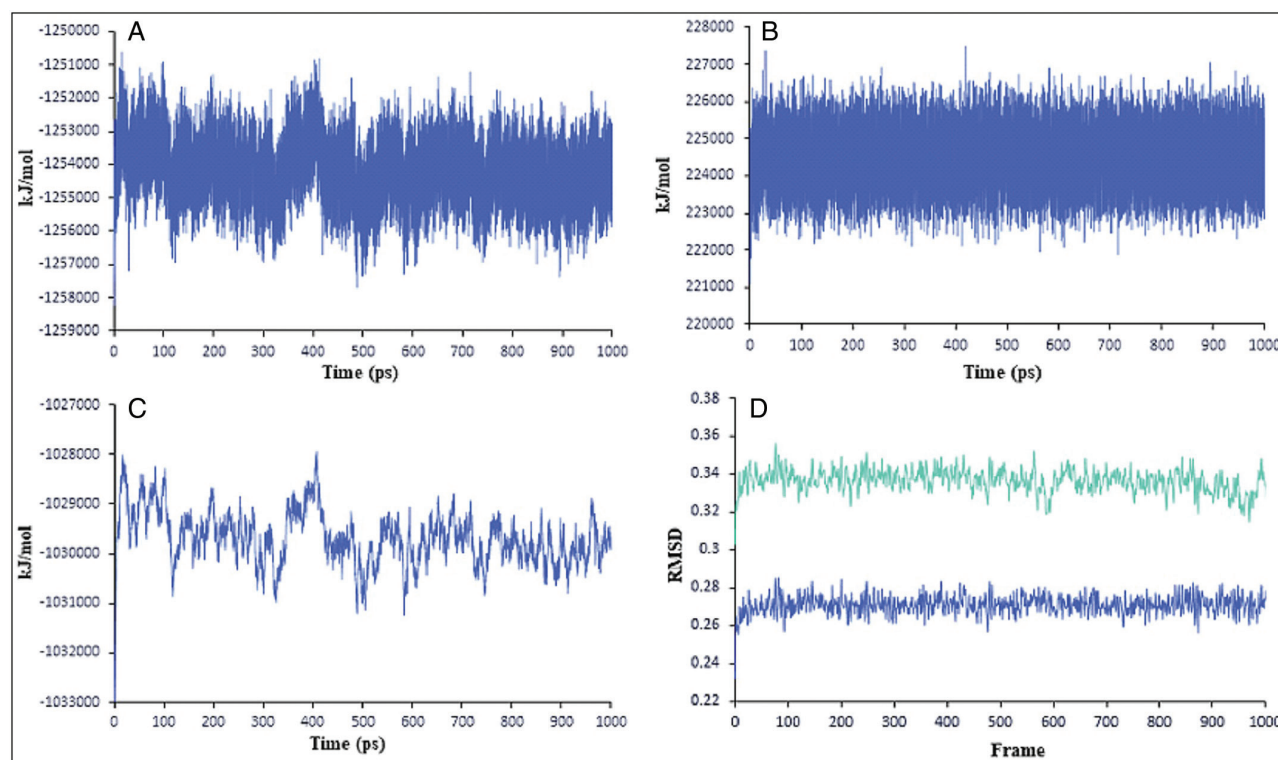


Figure 10: Analysis of MD trajectories for RdRp-indirubin complex (A) potential energy, (B) kinetic energy, (C) total energy and (D) RMSD of protein backbone (blue line) and system (green line)

Lipinski's filter includes molecular weight (MW) ≤ 500 , MLOGP (lipophilicity) ≤ 4.15 , number of hydrogen bond acceptors (HBA) ≤ 10 , and number of hydrogen bond donors

(HBD) ≤ 5 .^[24] Ritonavir and Lopinavir obey Lipinski's rules with 1 violation (MW>500), whereas two other control inhibitors, Sofosbuvir and Remdesivir violated 2 properties

Table 3: ADMET profile of the control inhibitors and the top docked compounds

Ligand	BBB+	GIA	P-gp Substrate	CYP2C9 inhibitor	HERG Inhibition	Carcinogens
Ritonavir	No	Low	Yes	No	Inhibitor	Non-carcinogens
Lopinavir	No	High	Yes	No	Inhibitor	Non-carcinogens
Sofosbuvir	No	Low	Yes	No	Weak inhibitor	Non-carcinogens
Remdesivir	No	Low	Yes	No	Weak inhibitor	Non-carcinogens
Indigo	Yes	High	No	No	Weak inhibitor	Non-carcinogens
Indirubin	Yes	High	No	No	Weak inhibitor	Non-carcinogens
Dihydroxyisopropylidenylisatisine A	No	High	No	No	Weak inhibitor	Non-carcinogens
Isatibisindosulfonic acid B	No	High	Yes	No	Weak inhibitor	Carcinogens

by having MW>500 and NorO>10. Indigo, Indirubin, Dihydroxyisopropylidenylisatisine A and Isatibisindosulfonic acid B are drug likeness without any violation.

TPSA or Topological Polar Surface Area indicates the surface belonging to polar atoms in the compound. An increased TPSA is associated with diminished membrane permeability and compounds with higher TPSA were better substrates for P-gp (responsible for drug efflux from cell). It was also predicted that a molecule with better CNS penetration should have lower TPSA value.^[37] TPSA for the alkaloids is lower than the control inhibitors. Indigo and Indirubin, both with TPSA of 65.45 Å² have ability to pass BBB [Tables 2 and 3].

However, others cannot cross from BBB. Among the compounds, Indigo, Indirubin and Dihydroxyisopropylidenylisatisine A are not substrate of P-gp. All the four alkaloids have high GI absorption, whereas among the control inhibitors, only Lopinavir has high intestinal absorption. None of the compounds act as CYP450 2C9 inhibitors that means they do not hamper the biotransformation of drugs metabolized by CYP450 2C9.^[37] In term of toxicity, Ritonavir and Lopinavir are inhibitor of HERG, whereas others are weak inhibitors. Inhibition of the HERG channel delays repolarization and prolongs the QT interval and cardiac action potential, which can lead to sudden death.^[38] All the compounds were indicated to be non-carcinogenic except Isatibisindosulfonic acid B [Table 3]. Overall, ADMET profiles of Indigo, Indirubin and, Dihydroxyisopropylidenylisatisine A are more favorable than others.

Discussion

Despite much effort, there is no effective treatment for SARS-CoV-2 infection yet. Discovering new effective drugs is very time consuming, therefore using computational methods that can speed up this process is beneficial. On the contrary, due to the high cost and the need to provide special laboratory conditions for anti-SARS-CoV-2 activities studies of natural products, the use of computer modeling studies is one of the most cost-effective methods to introduce anti-SARS-CoV-2 compounds for *in-vitro* and *in-vivo* studies in the future.^[39] Investigations showed the prominent antiviral activity of alkaloids by inhibiting enzymes vital for virus replication.^[40] Also, these compounds showed a high affinity for DNA, which is another reason to consider alkaloids as a promising candidate

against SARS-CoV-2.^[8] So, we computationally examined the interactions of 15 alkaloids of *Isatis indigotica* with three key enzymes of SARS-CoV-2 which have an important role in viral life cycle. Also in this study, the toxicity of the studied alkaloids has been predicted. Our results show that indole alkaloids collectively showed better binding affinity to PLpro, 3CLpro and RdRp than non-indole alkaloids containing sulfur group. Therefore, it can be said that higher affinity of these phytochemicals might be relevant to indole group. It is reported that indole derivatives can act as protease and polymerase inhibitors.^[41] It seems that the presence of two indole groups is more effective than one in the stability of these interactions. Because the ligands, which have two indole groups including Dihydroxyisopropylidenylisatisine A, Indigo, Indirubin, Isatibisindosulfonic acid B, Insatindibisindolamide A and Insatindibisindolamide B made stronger connections with the target proteins in compared with Indican and Isatindosulfonic acid B (having single indole group). Dihydroxyisopropylidenylisatisine A has highest affinity for both proteases; 3CLpro and PLpro (binding affinity: -8.5 and -9.3 kcal/mol, respectively). Hence, this compound might be potential therapeutic candidate against SARS-CoV2. Besides, Indigo showed acceptable binding affinity (-8.5 kcal/mol) for PLpro and interacted with the key residues of the active site. For RdRp, Indirubin was best compound among the phytochemicals that interacted with the active site residues, that is, Asp760 and Asp761 with higher affinity than Sofosbuvir and Remdesivir. Among all compounds, Epigotrin had lowest affinity toward PLpro, 3CLpro and RdRp which may be due to its small size. Also, molecular dynamics simulation study was performed for 1000 ps to analyze the stability of the best complexes. Based on potential and total energy, the 3CLpro-Dihydroxyisopropylidenylisatisine A system has the lowest amount of energy and shows the most stable state compare to the other two systems. These alkaloids also have desirable physicochemical and pharmacokinetic properties. Therefore, more investigation regarding the capability of these compounds recommended.

Conclusions

In this study, in order to evaluate anti-SARS-CoV-2 activity of several main alkaloids of *Isatis indigotica*, molecular docking was performed against 3CLpro, PLpro and RdRp. Our findings showed that Dihydroxyisopropylidenylisatisine

A with highest affinity bound to 3CLpro and interacted with the key residues in the active site. This complex has good stability, based on the molecular dynamics simulation results. Dihydroxylisopropylidenylisatisine A also was top-ranked ligand for PLpro. Therefore, it is thought that this compound may exert anti-SARS-CoV-2 effect through strong interactions with the active sites of these two viral proteases.

Financial support and sponsorship

Nil.

Conflicts of interest

There are no conflicts of interest.

References

- Sharma A, Tiwari S, Deb MK, Marty JL. Severe acute respiratory syndrome coronavirus-2 (SARS-cov-2): A global pandemic and treatment strategies. *Int J Antimicrob Agents* 2020;56:106054.
- Ianevski A, Yao R, Fenstad MH, Biza S, Zusinaite E, Reisberg T, *et al.* Potential antiviral options against SARS-CoV-2 infection. *Viruses* 2020;12:642.
- Mani JS, Johnson JB, Steel JC, Broszczak DA, Neilsen PM, Walsh KB, *et al.* Natural product-derived phytochemicals as potential agents against coronaviruses: A review. *Virus Res* 2020;284:197989.
- Majnooni MB, Fakhri S, Shokoohinia Y, Kiyani N, Stage K, Mohammadi P, *et al.* Phytochemicals: Potential therapeutic interventions against coronavirus-associated lung injury. *Front Pharmacol* 2020;11:588467.
- Ozcelik B, Kartal M, Orhan I. Cytotoxicity, antiviral and antimicrobial activities of alkaloids, flavonoids, and phenolic acids. *Pharm Biol* 2011;49:396-402.
- Houghton PJ, Woldemariam TZ, Khan AI, Burke A, Mahmood N. Antiviral activity of natural and semi-synthetic chromone alkaloids. *Antiviral Res* 1994;25:235-44.
- Kim DE, Min JS, Jang MS, Lee JY, Shin YS, Park CM, *et al.* Natural bis-benzylisoquinoline alkaloids-tetrandrine, fangchinoline, and cepharanthine, inhibit human coronavirus OC43 infection of MRC-5 human lung cells. *Biomolecules* 2019;9:696.
- Wink M. Potential of DNA intercalating alkaloids and other plant secondary metabolites against SARS-CoV-2 causing COVID-19. *Diversity* 2020;12:175.
- Chen J, Dong X, Li Q, Zhou X, Gao S, Chen R, *et al.* Biosynthesis of the active compounds of *isatis indigotica* based on transcriptome sequencing and metabolites profiling. *BMC Genomics* 2013;14:857.
- Meng L, Guo Q, Liu Y, Chen M, Li Y, Jiang J, *et al.* Indole alkaloid sulfonic acids from an aqueous extract of *isatis indigotica* roots and their antiviral activity. *Acta Pharm Sin B* 2017;7:334-41.
- Ho YL, Chang YS. Studies on the antinociceptive, anti-inflammatory and anti pyretic effects of *isatis indigotica* root. *Phytomedicine* 2002;9:419-24.
- Liu SF, Zhang YY, Zhou L, Lin B, Huang XX, Wang XB, *et al.* Alkaloids with neuroprotective effects from the leaves of *isatis indigotica* collected in the anhui province, china. *Phytochemistry* 2018;149:132-9.
- Zhang D, Shi Y, Li J, Ruan D, Jia Q, Zhu W, *et al.* Alkaloids with nitric oxide inhibitory activities from the roots of *Isatis tinctoria*. *Molecules* 2019;24:4033.
- Lin CW, Tsai FJ, Tsai CH, Lai CC, Wan L, Ho TY, *et al.* Anti-SARS coronavirus 3C-like protease effects of *isatis indigotica* root and plant-derived phenolic compounds. *Antiviral Res* 2005;68:36-42.
- Ghosh R, Chakraborty A, Biswas A, Chowdhuri S. Depicting the inhibitory potential of polyphenols from *Isatis indigotica* root against the main protease of SARS CoV-2 using computational approaches. *J Biomol Struct Dyn* 2020:1-12.
- Burley SK, Berman HM, Kleywegt GJ, Markley JL, Nakamura H, Velankar S. Protein Data Bank (PDB): The single global macromolecular structure archive. *Protein Crystallography. Methods in Molecular Biology*. New York: Humana Press; 2017. p. 627-41.
- BIOVIA DS. BIOVIA Discovery Studio Visualizer, v16. 1.0. 15350. San Diego: Dassault Systemes; 2015. [cited: 2017 Mar 20].
- Neese F, Wennmohs F. ORCA (3.0. 2)-An ab Initio. DFT and Semiempirical SCF-MO Package. Germany: Max-Planck-Institute for Chemical Energy Conversion Stiftstr 34-36, 45470 Mulheim ad Ruhr; 2013.
- Muhammad SA, Fatima N. In silico analysis and molecular docking studies of potential angiotensin-converting enzyme inhibitor using quercetin glycosides. *Pharmacogn Mag* 2015;11:S123-6.
- Wallace AC, Laskowski RA, Thornton JM. LIGPLOT: A program to generate schematic diagrams of protein-ligand interactions. *Protein Eng* 1995;8:127-34.
- Kaur S, Kulharia M. Insights from the molecular dynamics simulation of bcsd subunit from *K. Xylinus*. *Bioinformatics* 2017;13:376-9.
- Meduru H, Wang YT, Tsai JJ, Chen YC. Finding a potential dipeptidyl peptidase-4 (DPP-4) inhibitor for type-2 diabetes treatment based on molecular docking, pharmacophore generation, and molecular dynamics simulation. *Int J Mol Sci* 2016;17:920.
- Ranjith D, Ravikumar C. SwissADME predictions of pharmacokinetics and drug-likeness properties of small molecules present in *Ipomoea mauritiana* Jacq. *J Pharmacogn Phytochem* 2019;8:2063-73.
- Lipinski CA, Lombardo F, Dominy BW, Feeney PJ. Experimental and computational approaches to estimate solubility and permeability in drug discovery and development settings. *Adv Drug Deliv Rev* 1997;23:3-25.
- Cheng F, Li W, Zhou Y, Shen J, Wu Z, Liu G, *et al.* admetSAR: A comprehensive source and free tool for assessment of chemical ADMET properties. *J Chem Inf Model* 2012;52:3099-105.
- Amin SA, Ghosh K, Gayen S, Jha T. Chemical-informatics approach to COVID-19 drug discovery: Monte Carlo based QSAR, virtual screening and molecular docking study of some in-house molecules as papain-like protease (PLpro) inhibitors. *J Biomol Struct Dyn* 2021;39:4764-73.
- Kumar Y, Singh H, Patel CN. In silico prediction of potential inhibitors for the main protease of SARS-cov-2 using molecular docking and dynamics simulation based drug-repurposing. *J Infect Public Health* 2020;13:1210-23.
- Yang H, Yang M, Ding Y, Liu Y, Lou Z, Zhou Z, *et al.* The crystal structures of severe acute respiratory syndrome virus main protease and its complex with an inhibitor. *Proc Natl Acad Sci U S A* 2003;100:13190-5.
- Xu J, Zhang M, Lin X, Wang Y, He X. A steroidal saponin isolated from *Allium chinense* simultaneously induces apoptosis and autophagy by modulating the PI3K/akt/mTOR signaling pathway in human gastric adenocarcinoma. *Steroids* 2020;161:108672.
- Bagherzadeh K, Daneshvarnejad K, Abbasiazari M, Azizian H. In silico repositioning for dual inhibitor discovery of SARS-CoV-2 (COVID-19) 3C-like protease and papain-like peptidase. 2020. doi: 10.20944/preprints202004.0084.v1.
- Ahmad J, Ikram S, Ahmad F, Rehman IU, Mushtaq M. SARS-cov-2 RNA dependent RNA polymerase (rdp) - A drug repurposing study. *Heliyon* 2020;6:e04502.
- Vijayakumar BG, Ramesh D, Joji A, Jayachandra Prakasan J, Kannan T. In silico pharmacokinetic and molecular docking studies

- of natural flavonoids and synthetic indole chalcones against essential proteins of SARS-cov-2. *Eur J Pharmacol* 2020;886:173448.
33. Elfiky AA. Anti-HCV, nucleotide inhibitors, repurposing against COVID-19. *Life Sci* 2020;248:117477.
 34. Elfiky AA. Ribavirin, Remdesivir, Sofosbuvir, Galidesivir, and Tenofovir against SARS-CoV-2 RNA dependent RNA polymerase (RdRp): A molecular docking study. *Life Sci* 2020:117592.
 35. Rane JS, Pandey P, Chatterjee A, Khan R, Kumar A, Prakash A, *et al.* Targeting virus–host interaction by novel pyrimidine derivative: An in silico approach towards discovery of potential drug against COVID-19. *J Biomol Struct Dyn* 2021;39:5768-78.
 36. Gyebi GA, Ogunro OB, Adegunloye AP, Ogunyemi OM, Afolabi SO. Potential inhibitors of coronavirus 3-chymotrypsin-like protease (3clpro): An in silico screening of alkaloids and terpenoids from African medicinal plants. *J Biomol Struct Dyn* 2021;39:3396-408.
 37. Nisha CM, Kumar A, Nair P, Gupta N, Silakari C, Tripathi T, *et al.* Molecular docking and in silico ADMET study reveals acylguanidine 7a as a potential inhibitor of β -secretase. *Adv Bioinformatics* 2016;2016:9258578.
 38. Schramm A, Baburin I, Hering S, Hamburger M. HERG channel inhibitors in extracts of *Coptidis rhizoma*. *Planta Med* 2011;77:692-7.
 39. Aminpour M, Montemagno C, Tuszynski JA. An overview of molecular modeling for drug discovery with specific illustrative examples of applications. *Molecules* 2019;24:1693.
 40. Majnooni MB, Fakhri S, Bahrami G, Naseri M, Farzaei MH, Echeverria J. Alkaloids as potential phytochemicals against SARS-cov-2: Approaches to the associated pivotal mechanisms. *Evid Based Complement Alternat Med* 2021;2021:6632623.
 41. Zhang MZ, Chen Q, Yang GF. A review on recent developments of indole-containing antiviral agents. *Eur J Med Chem* 2015;89:421-41.